Dynamic magnetic response across the pressure-induced structural phase transition in CeNi

A. Mirmelstein,[1] A. I. Kolesnikov,[2] G. Ehlers,[3] D. L. Abernathy,[2] V. Matvienko,[1] A. S. Sefat,[4] and A. Podlesnyak[2,*]

[1]*Russian Federal Nuclear Center - E.I. Zababakhin Research Institute of Technical Physics, 13 Vasiliev str., 456770 Snezhinsk, Russia*
[2]*Neutron Scattering Division, Oak Ridge National Laboratory, Oak Ridge, Tennessee 37831, USA*
[3]*Neutron Technologies Division, Oak Ridge National Laboratory, Oak Ridge, Tennessee 37831, USA*
[4]*Materials Science and Technology Division, Oak Ridge National Laboratory, Oak Ridge, Tennessee 37831, USA*

The intermediate-valence compound CeNi experiences a pressure-induced first-order structural phase transition with an abrupt change in the unit cell volume, and as such constitutes an attractive system to study pressure-driven f-electron delocalization behavior in a system with an unstable f-electron shell. The inelastic neutron scattering study of the dynamic magnetic response of CeNi reveals that the structural transition increases the characteristic energy of magnetic fluctuations due to enhanced Ce $4f$–Ni $3d$ hybridization. At the same time, the inelastic $4f$ magnetic form factor remains unchanged.

I. INTRODUCTION

Pressure-induced first-order structural phase transitions accompanied by abrupt volume variations are a very remarkable phenomenon in the physics of strongly correlated electron systems. Such a phenomenon is usually explained in relation to a crossover between localized and itinerant f-electron behavior in rare-earth- or actinide-based materials. The most studied example of such a phase transition is the isostructural volume collapse transition in cerium metal, first reported in 1927 by Bridgman [1]. Since 1949, when the isostructural nature of the $\gamma \rightarrow \alpha$ transition was established [2], it stimulated a lot of experimental and theoretical work aimed to explain the large isostructural volume change of $\sim 15\%$ as well as the replacement of the normal Curie-Weiss temperature dependence in the magnetic susceptibility of the γ phase, which is indicative of a local moment behavior, by a practically temperature independent susceptibility in α-Ce [3], suggesting a quenched moment state. In spite of the long history, the nature of this transition is still actively discussed [4–6]. An even more intriguing example of such a transition in an f-electron system is the $\delta \rightarrow \alpha$ transformation in plutonium metal [7]. Recent remarkable Inelastic Neutron Scattering (INS) experiments clearly demonstrate that plutonium metal also has a valence-fluctuating ground state [8]. Nevertheless, many features of structural transformations in Pu still have no explanation, including the stabilization of the face-centered-cubic (fcc) phase by alloying different elements, or the influence of defects and strain on the transformation. Details of the variation of the Pu f-electron configuration at the transition are also unknown.

INS is a key experimental technique to study strongly correlated f-electron systems, and in particular the phenomenon of the volume collapse transitions. The first INS investigations of this phenomenon were performed by Shapiro *et al.* [9]

and Loong *et al.* [10]. They studied the magnetic excitation spectrum of the mixed-valence alloy $Ce_{0.74}Th_{0.26}$. A shift in the spectral weight was found from quasielastic scattering in the high-temperature γ-phase into a broad inelastic signal in the low-temperature α-phase. The increase in the width of the magnetic response of almost an order of magnitude in the α phase was interpreted as a result of a sudden increase of the hybridization involving f- and conduction electrons due to the $\gamma \rightarrow \alpha$ transition [10]. These experiments also showed that the magnetic form factor F(**Q**) (**Q** is the scattering vector) does not change at the transition and that, for both the γ and α phases, it follows the **Q** dependence predicted for the Ce^{3+} $4f$ free ion with the total $4f$ shell angular momentum $J = 5/2$. This was later confirmed for the α phase with higher precision by Murani *et al.* [11]. The temperature variation of the PDOS of $Ce_{0.9}Th_{0.1}$ was later studied at temperatures from 10 to 300 K by Manley *et al.* [12]. The net result of these INS measurements was that the $\alpha \rightarrow \gamma$ transition in this alloy is purely driven by electronic degrees of freedom.

The behavior of the magnetic response observed in the INS measurements [10] is consistent with the interpretation in terms of the Kondo-Anderson single-impurity (K/AI) model [13–16]. The K/AI model provides a satisfactory description of the physical properties of a large number of intermediate-valence (IV) polycrystalline systems, where the localized $4f$ electrons occupy the regular sites of the crystal lattice (see Ref. [17] and references therein). According to this model, in the IV state the hybridization of the $4f$ wave functions with conduction band states is large, causing the suppression of sharp crystal-field excitations and the appearance of a strongly damped, featureless magnetic response. At low temperatures, the **Q**-averaged magnetic neutron spectrum is typically dominated by one broad inelastic peak centered at an energy of several tens to some hundreds of meV related to the characteristic energy scale $E_0 = k_B T_K$, where T_K is the Kondo temperature. When the temperature is increased, the spectral weight is gradually transferred to a quasielastic line, corresponding to the regime of local magnetic moments.

*Corresponding author: podlesnyakaa@ornl.gov

The applicability of the K/AI model to these materials can be understood as a result of the highly localized nature of the $4f$ spin fluctuations. However, recent INS measurements of the dynamic magnetic susceptibility of $CePd_3$ single crystals by Fanelli *et al.* [18] and Goremychkin *et al.* [19] showed that at low temperatures well below T_K coherent effects develop, resulting in the formation of a coherently hybridized f-spd band, and, as a consequence, the magnetic response becomes strongly momentum dependent.

Years ago, very strong coherent effects were also observed in the IV compound CeNi [20]. CeNi has the CrB-type orthorhombic crystal structure (space group $Cmcm$) [21], repeatedly appearing in rare-earth and actinide metals under pressure such as α'-Ce, Pa, Nd, and Pr. The α-U phase also has this type of structure which is usually stable up to very high pressure. CeNi shows different behavior. Already at ambient pressure, CeNi displays clear signatures of a lattice instability upon cooling [22]. However, a structural transformation with abrupt volume change only occurs under the application of external pressure, albeit relatively low [23–25]. Nevertheless, the structure of the CeNi high pressure phase remained unknown for a long time. Recently, we performed detailed x-ray and neutron powder-diffraction experiments to study this transition in CeNi and showed that the structure of the pressure-induced phase can be described in terms of the $Pnma$ space group [26]. Equations of state of CeNi on both sides of the phase transition were derived and an approximate P-T phase diagram was suggested for $P < 8$ GPa and $T < 300$ K. The observed $Cmcm \rightarrow Pnma$ structural transition was analyzed using density functional theory calculations, which successfully reproduced the ground state volume, the phase transition pressure, and the volume collapse associated with the phase transition. We concluded that the decrease of the Ce-Ni interatomic distances suggests an enhanced Ce $4f$–Ni $3d$ hybridization in the high-pressure CeNi phase as compared to the ambient pressure CeNi structure. As a result, one can expect an increase of the characteristic magnetic fluctuation energy T_K in the high-pressure $Pnma$ phase. However, to achieve a more direct and complete understanding of the evolution of the $4f$ electronic states across the volume-collapse transition, INS experiments are required.

According to the INS measurements of the dynamic magnetic susceptibility for the polycrystalline $Ce^{60}Ni$ sample [20,27], the magnetic intensity essentially vanishes at energies below 15 meV, indicating a spin-gap-like response. This is a clear evidence for the formation of a singlet ground state due to electron correlations. At higher energies, the magnetic response of the polycrystalline $Ce^{60}Ni$ can be described by an inelastic Lorentzian centered at $E = 33 \pm 3$ meV and $\Gamma/2 = 45 \pm 5$ meV, where Γ is the full width at half maximum (FWHM). For the single crystal of $Ce^{60}Ni$, however, at $E > 15$ meV the magnetic response consists of a broad structureless contribution, typical for valence-fluctuating materials, and two additional narrow peaks at about 18 and 34 meV, whose intensities vary as a function of both the reduced wave vector and the direction in reciprocal space [20]. At the present time, the origin of these coherent features in the CeNi INS spectrum remains unexplained. Obviously, they cannot be described in terms of the K/AI model, like the coherent effects in $CePd_3$ [18,19]; however, we have no arguments to

say whether these effects have a similar origin in the two systems or not. Thus, the aim of this paper is to study, using the INS technique, the variation of the magnetic excitation spectrum in CeNi across the pressure-induced structural phase transition.

II. EXPERIMENTAL DETAILS

The polycrystalline CeNi sample of ~ 3 g in mass for INS experiments was prepared using ^{60}Ni isotope (enrichment 99%). This isotope has nuclear scattering cross section $\sigma_S = 1.0$b, as compared to $\sigma_S = 18.5$b for the natural isotopic composition. The reduction of nuclear scattering from Ni atoms by almost a factor of 20 makes it possible to extract the weak magnetic contribution from Ce atoms (magnetic cross section of Ce^{3+} ions is $\sigma_M \sim 3.7$b [27]) with sufficient reliability and accuracy. Stoichiometric amounts of elemental reactants, Ce (chunks, Ames) and ^{60}Ni (Trace Sciences International Corporation) were loaded into alumina crucibles, which were baked at $800\,^{\circ}$C prior to use, and then put inside quartz tubes. Alumina crucibles containing Zr pieces were placed on top as potential oxygen sponges during the sample synthesis process. Quartz tubes were sealed under vacuum, and subsequently heated inside box furnaces at $800\,^{\circ}$C for 6 h, followed by $1\,^{\circ}$C/h, cooling to $600\,^{\circ}$C. The phase purity of the synthesized samples was verified using x-ray powder diffraction and magnetization measurements. The diffraction experiment revealed the CrB-type structure ($Cmcm$ space group) with a small amount of an impurity phase ($<2\%$ of $CeNi_2$). Magnetization measurements performed with a commercial Physical Properties Measurement System (Quantum Design) showed good agreement with the published data as it will be discussed below.

To generate pressure in the INS experiments, we used an Al alloy pressure cell with He gas as a pressure transmitting medium. Measurements of the INS spectra of $Ce^{60}Ni$ were performed using the fine-resolution Fermi chopper spectrometer SEQUOIA (Spallation Neutron Source at Oak Ridge National Laboratory) [28,29] at temperature 22 K. A bottom-loading closed cycle refrigerator (CCR) was used to cool the sample. The incident neutron energy was $E_i = 150$ meV, resulting in an energy resolution of Gaussian shape with FWHM 3.6 meV at the elastic line. To measure the magnetic form factor of $Ce^{60}Ni$, we used the ARCS [30] (wide angular-range chopper spectrometer) instrument (Spallation Neutron Source at Oak Ridge National Laboratory). ARCS allows one to measure the inelastic spectra at the same incident neutron energy $E_i = 150$ meV (energy resolution at the elastic line ~ 6 meV) up to a high momentum transfer $|\mathbf{Q}| \sim 12$Å^{-1} within the energy transfer region 50–80 meV.

To separate the magnetic contribution from the measured inelastic signal, the experimental data were carefully treated taking into account the background from the pressure cell as well as the helium pressure transmitting medium. To do this, we measured the empty pressure cell with He gas under pressure and the sample without pressure cell, all at $T = 22$ K. The phonon contribution was determined using the experimental data for sufficiently large momentum transfer Q, where there is no magnetic contribution to the scattering. The precise measurements of the background contributions allow
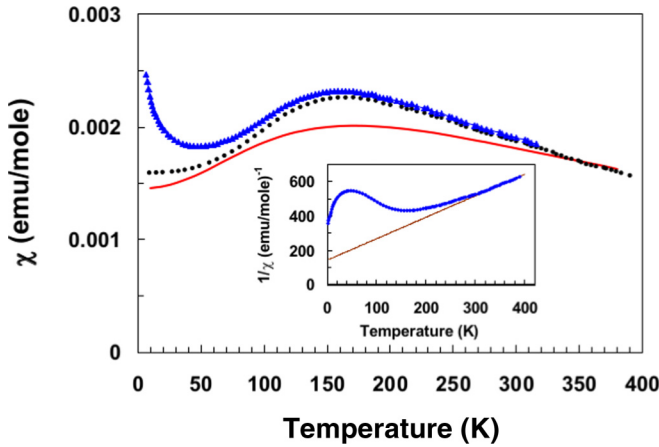
FIG. 1. Temperature dependence of the magnetic susceptibility for the $Ce^{60}Ni$ sample synthesized for the INS measurements (blue triangles). The solid red line shows the spin-fluctuating contribution to the susceptibility calculated according to the Coqblin-Schrieffer model [31] with $E_0 = 31$ meV. The dotted curve shows the difference between the measured $Ce^{60}Ni$ susceptibility χ_{exp} and the low-temperature Curie-Weiss type contribution χ_{C-W}, which has, at least partially, an intrinsic origin (see text). The inset shows an inverse magnetic susceptibility $1/\chi$ as a function of temperature (blue rhombus). The straight line shows the inverse Curie-Weiss susceptibility for the Ce^{3+} free ion Curie constant $C_{5/2}$.

us to reliable isolate the magnetic part over a wide range of momentum transfer.

The pressure cell with He gas as transmitting medium was used as it allowed to adjust the pressure while cooling the sample. The large thermal contraction of CeNi and the volume change at the transition make this necessary. In a clamp cell, without *in situ* adjustment of the pressure, the actual pressure would drop too much at low temperature.

III. MAGNETIC EXCITATION SPECTRUM

As mentioned above, CeNi is an IV system. According to the x-ray absorption spectroscopy data, the Ce valence increases from ~3.11 to 3.14 under cooling from 300 K down to ~20 K [32]. Generally, the temperature dependent susceptibility χ shows a broad maximum around 150 K which is typical for an IV system. At the same time, CeNi displays strong magnetic anisotropy, so that this characteristic shape of the χ vs temperature curve is much more pronounced in a magnetic field applied along the c axis of the orthorhombic structure than along the a and b directions [33]. The absolute values and temperature dependence of the magnetic susceptibility for our $Ce^{60}Ni$ sample (Fig. 1) agrees with the published data [33]. At $T > 300$ K χ follows the Curie-Weiss law with the free Ce^{3+} ion effective moment $p = g[(J(J+1)]2 = 2.53$, $J = 5/2$ (inset in Fig. 1). At low temperatures, the contribution to χ due to spin fluctuations is approximately temperature independent, and the anomalous upturn of $\chi(T)$ below 30 K has, at least partially, an intrinsic origin presumably connected with coherent $f - d$ hybridization [18,34]. Spin-fluctuating (or impurity) contribution to the magnetic susceptibility of our $Ce^{60}Ni$ sample (dotted line in Fig. 1, obtained as a
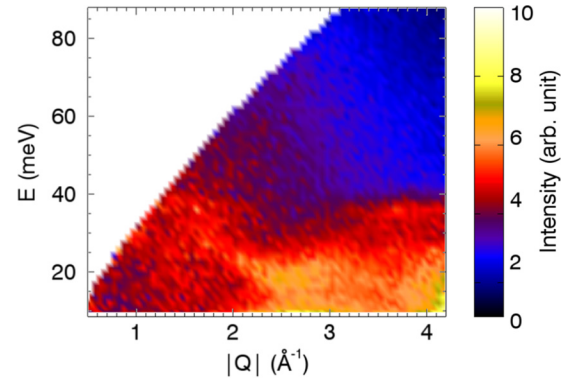

FIG. 2. Contour plot of a raw INS spectrum for $Ce^{60}Ni$ sample at ambient pressure and $T = 22$ K. Phonon acoustic waves of aluminum from the sample container are clearly visible (see text).

difference $\chi_{exp} - \chi_{C-W}$) can be well approximated in terms of Coqblin-Schrieffer model [31] with the characteristic energy $E_0 = 31 \pm 1$ meV (red line in Fig. 1).

A typical INS spectrum of $Ce^{60}Ni$ is shown in Fig. 2. The broad INS intensity at low $|\mathbf{Q}|$ is clearly visible below 3 Å^{-1}. The rapid drop of intensity at large $|\mathbf{Q}|$ is an indication of the magnetic origin of the excitation. The intensity with the origin at $|\mathbf{Q}| \sim 2.5$ Å^{-1} is mainly due to Al phonon contributions.

Figure 3 shows the magnetic scattering function $S_M(E, T = 22K)$ for $Ce^{60}Ni$ measured at 22 K and ambient pressure. To decrease background nuclear scattering, the sample was not placed into a pressure cell for this measurement. After nuclear background subtraction, the magnetic inelastic signal was averaged over all scattering vector $\mathbf{Q}$ directions and then summed up within the $|\mathbf{Q}|$ interval 1.5 to 4 Å^{-1}. For higher $|\mathbf{Q}|$, the magnetic signal is suppressed by a sharp decrease of the magnetic form factor [35]. One can immediately see that the obtained inelastic spectrum looks very similar to that reported for a $Ce^{60}Ni$ single crystal in Ref. [20]. To describe $S_M(E, T = 22K)$ the standard expression was used:

$$S_M(\mathbf{Q}, E, T) \sim |F(\mathbf{Q})|^2 \cdot \frac{E}{1 - \exp\{-E/k_B T\}}$$
$$\times \frac{\Gamma/2}{(\Gamma/2)^2 + (E - E_0)^2}, \quad (1)$$

where Γ is the FWHM of the Lorentzian spectral component. The energy E_0 determines the characteristic energy scale of the IV system, i.e., the Kondo temperature $T_K = E_0/k_B$.

As seen from Fig. 3, three Lorentzian functions are required to describe the measured $S_M(E, T = 22K)$, namely, two very narrow and one broad with the parameters: $E_{01} = 15 \pm 0.2$ meV, $\Gamma/2 = 3.3 \pm 0.2$ meV, $E_{02} = 30 \pm 0.3$ meV, $\Gamma/2 = 3.3 \pm 0.2$ meV, $E_{03} = 40 \pm 2$ meV, $\Gamma/2 = 42 \pm 3$ meV. These parameters are very close to those found for the $Ce^{60}Ni$ single crystal in Ref. [20]: $E_{01} \sim 18$ meV, $\Gamma/2 = 4.5 \pm 0.5$ meV, $E_{02} \sim 34$ meV, $\Gamma/2 = 4.5 \pm 0.5$ meV, $E_{03} \sim 46$ meV, $\Gamma/2 = 24$ meV.

Thus, our results demonstrate quantitative agreement with the data reported in Ref. [20]. According to the $|\mathbf{Q}|$ dependence of our data, all three spectral components are presumably of magnetic origin. It should be noted, however,
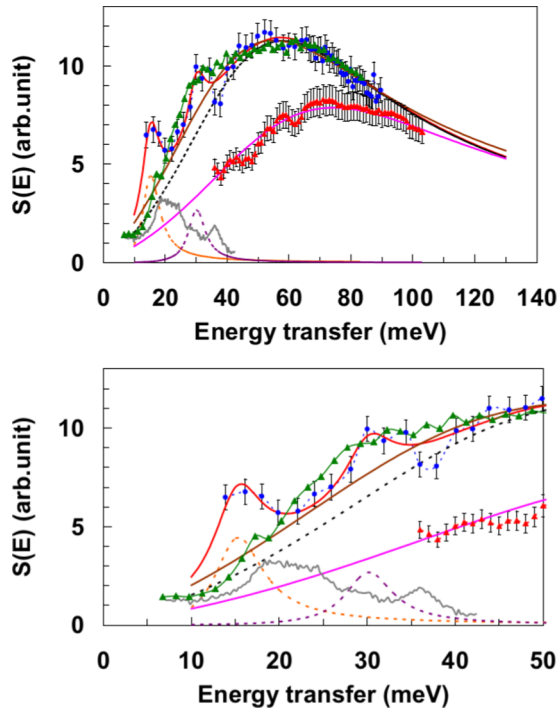
FIG. 3. Top: Magnetic scattering function $S_M(E)$ for the $Ce^{60}Ni$ sample at ambient pressure (before the structural transition, blue circles) and at pressure $P = 0.4$ GPa (after the transition, red triangles). Both spectra were measured at $T = 22$ K using the SEQUOIA spectrometer. The dashed lines show a fit of the experimental magnetic spectrum at ambient pressure by three inelastic Lorentzian functions E_1, E_2, E_3 (see text). The sum of the E_1, E_2, E_3 spectral contributions is shown by the red curve. The solid brown curve is the result obtained for $S_M(E)$ in Ref. [27] and solid lilac curve shows a fit by a single Lorentzian of the experimental scattering function $S_M(E)$ measured at $P = 0.4$ GPa. Green triangles represent $S_M(E)$ for the $Ce^{60}Ni$ sample at ambient pressure measured at $T = 22$ K at ARCS without pressure cell. The sample measured was the same as on the SEQUOIA measurements, but after direct $Cmcm \rightarrow Pnma$ and inverse $Pnma \rightarrow Cmcm$ structural phase transitions. Phonon density of states for aluminum is also indicated by dashed grey line. Bottom: The same scattering functions for $Ce^{60}Ni$ in the energy range of 10–50 meV. Orange, violet, and black dashed lines correspond to the three inelastic Lorentzian functions E_1, E_2, E_3, respectively.

that the maxima of the Al phonon density of states (PDOS) is at almost the same energies, ∼20 meV and 36 meV, as the sharp spectral lines E_{01} and E_{02} (Fig. 3). As a result, even a very small error in subtracting the nuclear inelastic background due to Al would have a dramatic influence on the intensities of these narrow features of the $S_M(E)$ function. Therefore, we cannot discuss the |**Q**| dependence of these spectral features in detail. Nevertheless, extremely low widths of the E_{01} and E_{02} lines provide clear evidence for the coherent nature of these spectral features, confirming the results of Ref. [20]. For a comparison, we plot in Fig. 3 $S_M(E)$ (solid brown curve) in the form of a single Lorentzian line with the parameters $E_0 = 33$ meV and $\Gamma/2 = 44$ meV obtained for the polycrystalline $Ce^{60}Ni$ sample [27]. This function describes the measured magnetic spectrum for our $Ce^{60}Ni$ sample rather well, excluding two narrow peaks which

were almost invisible in $S_M(E)$ in Ref. [27] (see Fig. 2 in Ref. [27] and Fig. 5 in Ref. [20]). The clear observation of the narrow peaks E_{01} and E_{02} in our measurements may also be the result of some texture (preferred orientation) in our sample. Note also that the Kondo energy $E_0 = 33$ meV agrees well with the value $E_0 = 31 \pm 1$ meV derived from the fit of magnetic susceptibility (Fig. 1). Thus, impressive similarity of the $S_M(E)$ general shapes and close values of the energy parameters of the $S_M(E)$ spectral components obtained in the present experiment and in Refs. [20,27], as well as a specific |**Q**| dependence of the E_{01} and E_{02} spectral line[1] allows us to conclude that the procedure to subtract nuclear background (which is the sum of $Ce^{60}Ni$ phonon contribution including multiple scattering and nuclear scattering by Al surrounding the sample) is correct, so that $S_M(E)$ in Fig. 3 represents the true magnetic scattering function of the CeNi system in the orthorhombic *Cmcm* structure.

To measure the dynamic magnetic response of CeNi after the structural transition, we performed the INS experiment at $T = 22$ K and $P = 0.4$ GPa using the top-loading He cryostat. In this case, the CeNi sample is surrounded by massive amounts of Al (material of the pressure cell) and He (pressure transmitting medium which gives a large inelastic signal), so that the nuclear background strongly increases as compared to the case of measurements at ambient pressure (note also that helium cryostat has larger background compared to the CCR). As a result, nuclear scattering dominates the inelastic spectrum at low energies, so that the accurate separation of weak magnetic contribution becomes a very difficult task unsolvable at the energy transfer below ∼40 meV. Unfortunately, this makes it impossible, at present, to follow the behavior of the two narrow peaks in the magnetic scattering function under pressure. Above an energy transfer $E \sim 40$ meV, the magnetic scattering function $S_M(E)$ of CeNi after the structural $Cmcm \rightarrow Pnma$ transition can be described by a Lorentzian with the parameters $E_0 = 50$ meV and $\Gamma/2 = 55$ meV (Fig. 3). Therefore, the structural transition accompanied by volume jump ($\Delta V/V \sim 8\%$ at low temperatures [26]) results in the increase in characteristic energy scale of magnetic fluctuations (Kondo temperature) while their lifetime decreases; that is, fluctuations dissipate faster than at ambient pressure.

The results obtained allow us to make some rough estimates. It was shown that for Ce-based materials with an unstable $4f$ shell the effective $4f$ occupation $\langle n_f \rangle$ and the Kondo energy E_0 are connected by an empirical relation [36]:

$$\langle n_f \rangle \approx 1 - 0.005(\text{meV}^{-1}) \times E_0. \qquad (2)$$

If $E_0 = 33$ meV at ambient pressure (single Lorentzian fit of magnetic scattering function), Eq. 2 gives $\langle n_f \rangle \approx 0.84$ (corresponding to the Ce ion valence 3.16, in agreement with [32]). At $P = 0.4$ GPa (after the transition) $E_0 = 50$ meV and $\langle n_f \rangle \approx 0.75$ (the Ce ion valence is 3.25). The electronic specific heat coefficient γ and the value of the Pauli-like

---

[1]Analysis of the obtained magnetic spectrum indicates irregular |**Q**|-dependence of the magnetic intensity around 30 meV with a maximum at $2.5 < |\mathbf{Q}| < 3$ Å^{-1}.

magnetic susceptibility of IV systems at low temperatures are proportional to $\langle n_f \rangle$ and inversely proportional to E_0 (see Ref. [37] and references therein):

$$\gamma, \chi_0 \propto \langle n_f \rangle / E_0. \qquad (3)$$

Therefore, our INS results give

$$\frac{\gamma(P=0)}{\gamma(P=0.4\text{GPa})} \approx \frac{\chi_0(P=0)}{\chi_0(P=0.4\text{GPa})}$$

$$\approx \frac{(\langle n_f \rangle / E_0)_{p=0}}{(\langle n_f \rangle / E_0)_{p=0.4\text{GPa}}} \approx 1.68. \qquad (4)$$

This value can be compared with the experimental data obtained by bulk measurements. From Ref. [25], the ratio $\chi_0(T=30\text{ K}, P=0)/\chi_0(T=30\text{ K}, P=0.47\text{ GPa}) = 0.00195/0.0015 \approx 1.30 \pm 0.05$[2]. A close value of the ratio $\gamma(P=0)/\gamma(P=0.4\text{ GPa}) \approx 1.36$ follows from the CeNi specific heat measurements under pressure [38]. It is worth noting that if one takes the value of $E_0 = 40$ meV (the energy of the broad peak E_{03} in Fig. 3) to Eq. (4) as a characterization of the initial CeNi state instead of single Lorentzian energy $E_0 = 33$ meV, then the $4f$ occupation at ambient pressure decreases down to $\langle n_f \rangle \approx 0.8$ and the ratio Eq. (4) acquires the value $\chi_0(P=0)/\chi_0(P=0.4\text{ GPa}) = 1.33$, equal to those from bulk measurements. Thus, three different experimental methods, which studied three different CeNi samples, give the consistent result characterizing the variation of CeNi electronic properties under the structural $Cmcm \rightarrow Pnma$ transition with the volume jump. The experimental results show clearly that the Kondo temperature increases in the compressed state as a result of the enhanced Ce $4f$–Ni $3d$ hybridization while the effective $4f$ shell occupation ($4f$ count) decreases. Note that the enhanced $4f$–$3d$ hybridization after the transition also follows from our structural results and *ab initio* CeNi electronic structure calculations [26]. Therefore, similar to the case of metallic cerium [4–6,9,10], the interaction between $4f$ electrons of Ce and the conduction band electrons plays a key role in the mechanism of the volume-collapse structural transition in CeNi.

IV. MAGNETIC FORM FACTOR

The analysis of the magnetic contribution from the measured INS spectrum shows that within the energy transfer range between ∼55 and 85 meV, i.e., around the $S_M(E)$ maximum, nuclear contributions become negligible. In other words, independently of the experimental conditions (measurements without pressure cell at ambient pressure or under pressure $P = 0.4$ GPa using the pressure cell), the measured inelastic signal is formed by the magnetic contribution plus some weak background almost independent of the momentum

---

[2]The pressure value $P = 0.47$ GPa is the result of cooling the pressure cell with CeNi sample down to 30 K if the applied pressure at room temperature was as high as 0.8 GPa [25] The value $\chi_0(T = 30\text{ K}, P = 0) = 0.00195$ emu/mole is the difference between measured value and low-temperature Curie-Weiss type contribution, i.e., this is the result of the similar procedure as shown by dotted line in Fig. 1.
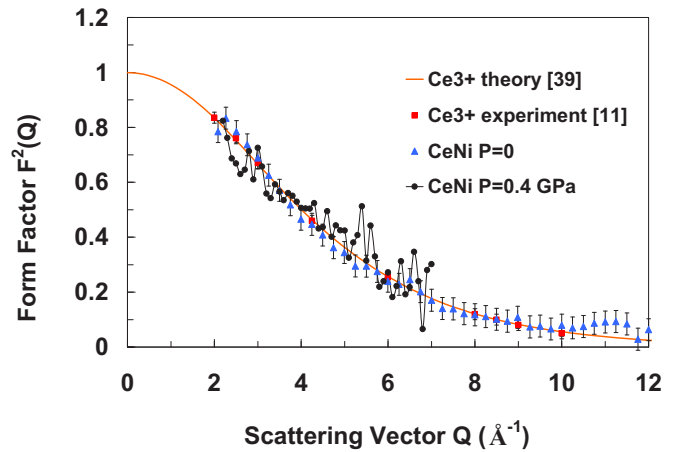
FIG. 4. Magnetic form factor $F^2(Q)$ of CeNi before (blue triangles) and after (black circles) pressure-induced volume-collapse structural phase transition. The calculated form factor for the free Ce^{3+} [39] and form factor measured experimentally for α-phase of metallic cerium [11] are shown for comparison.

transfer **Q**. Therefore, an experimental determination of the CeNi magnetic form factor $F(\mathbf{Q})$ before and after the structural transition becomes possible.

The INS measurements to determine the magnetic form factor were performed using the ARCS instrument with the incident neutron energy $E_i = 150$ meV in a wider momentum transfer $|\mathbf{Q}|$ range up to ∼12Å^{-1}. The same Ce^{60}Ni sample was used as in the experiments on SEQUOIA. The difference with the SEQUOIA experiment is that the sample did undergo direct $Cmcm \rightarrow Pnma$ and inverse $Pnma \rightarrow Cmcm$ structural phase transitions. To ensure that the direct and inverse structural transitions did not change the initial state of the sample, we measured first the sample in a CCR without pressure cell. The magnetic contribution extracted from the measured INS intensity was found to be in excellent agreement with the SEQUOIA result (Fig. 3). One can note, however, that both narrow spectral features are somewhat blurred as compared to the spectrum measured on SEQUOIA. This effect seems to be a natural sequence of the phase transitions, resulting in weakening of the preferred orientation (sample texture), and the coarse energy resolution of ARCS. Then the sample was installed in the same pressure cell as was used for the measurements on SEQUOIA and the INS spectrum was measured at the temperature 22 K and pressure 0.4 GPa. To determine the form factor, the measured spectra were first summed up over all the Q directions for each $|\mathbf{Q}|$, giving the functions $S_M(E, |\mathbf{Q}|)$. Then these $S_M(E, |\mathbf{Q}|)$ function were integrated within the energy window 60–80 meV, providing the intensity vs $|\mathbf{Q}|$ dependence (Fig. 4).

The results obtained demonstrate that the intensity of dynamic magnetic response of CeNi (to be exact, of broad incoherent spectral component) follows the free ion Ce^{3+} magnetic form factor before and after the structural transition in spite of an essential variation of Kondo temperature and spectral response broadening. Again, as in the case of the $\gamma \rightarrow \alpha$ transition in cerium [10,11], $4f$ electrons remain correlated, while strongly hybridized with conducting bands, in the CeNi $Pnma$ structure.

V. CONCLUSIONS

The dynamic magnetic response of the IV compound CeNi, before and after a pressure-induced volume-collapse structural phase transition, has been studied by INS. The experimental results clearly demonstrate the increase of the characteristic energy scale of magnetic fluctuations (Kondo temperature) and the decrease of the effective occupation in the $4f^1 (J = 5/2)$ ground state of the collapsed phase, due to the enhanced Ce $4f$–Ni $3d$ hybridization. It follows from the determination of magnetic form factor that the spatial distribution of the electronic density in the $4f$ shell does not change at the transition and remains the same as in the free Ce^{3+} ion. Thus, we may conclude that the behavior of the CeNi physical properties under pressure-induced structural phase transition follows the Kondo-Anderson impurity model and that the f electron delocalization is reflected by an increase of the Kondo temperature, or, in other words, by an increase of the low temperature many-particle resonance bandwidth.

[1] P. W. Bridgman, The compressibility and pressure coefficient of resistance of ten elements, Proc. Am. Acad. Arts Sci. **62**, 207 (1927).

[2] A. W. Lawson and Ting-Yuan Tang, Concerning the high pressure allotropic modification of cerium, Phys. Rev. **76**, 301 (1949).

[3] D. C. Koskenmaki and K. A. Gschneidner, Cerium, in *Handbook on the Physics and Chemistry of Rare Earths*, edited by K. A. Gschneidner and L. R. Eyring (North-Holland, Amsterdam, 1978), Vol. 1, Chap. 4, pp. 337–377.

[4] N. Lanatà, Y.-X. Yao, C.-Z. Wang, K.-M. Ho, J. Schmalian, K. Haule, and G. Kotliar, $\gamma - \alpha$ Isostructural Transition in Cerium, Phys. Rev. Lett. **111**, 196801 (2013).

[5] B. Chakrabarti, M. E. Pezzoli, G. Sordi, K. Haule, and G. Kotliar, α-γ transition in cerium: Magnetic form factor and dynamic magnetic susceptibility in dynamical mean-field theory, Phys. Rev. B **89**, 125113 (2014).

[6] N. Lanatà, Y.-X. Yao, C.-Z. Wang, K.-M. Ho, and G. Kotliar, Interplay of spin-orbit and entropic effects in cerium, Phys. Rev. B **90**, 161104 (2014).

[7] S. S. Hecker, Plutonium and its alloys—from atoms to microstructure, in *Challenge in Plutonium Science*, edited by N. G. Cooper (Los Alamos Science, Los Alamos, New Mexico, 2000), Vol. 2, No. 26, p. 290.

[8] M. Janoschek, P. Das, B. Chakrabarti, D. L. Abernathy, M. D. Lumsden, J. M. Lawrence, J. D. Thompson, G. H. Lander, J. N. Mitchell, S. Richmond, M. Ramos, F. Trouw, J.-X. Zhu, K. Haule, G. Kotliar, and E. D. Bauer, The valence-fluctuating ground state of plutonium, Sci. Adv. **1**, e1500188 (2015).

[9] S. M. Shapiro, J. D. Axe, R. J. Birgeneau, J. M. Lawrence, and R. D. Parks, Spin dynamics in the mixed valence alloy $Ce_{1-x}Th_x$, Phys. Rev. B **16**, 2225 (1977).

[10] C.-K. Loong, B. H. Grier, S. M. Shapiro, J. M. Lawrence, R. D. Parks, and S. K. Sinha, Neutron scattering studies of the paramagnetic response in the mixed-valence alloy $Ce_{1-x}Th_x$ at high energy, Phys. Rev. B **35**, 3092 (1987).

[11] A. P. Murani, S. J. Levett, and J. W. Taylor, Magnetic Form Factor of α-Ce: Towards Understanding the Magnetism of Cerium, Phys. Rev. Lett. **95**, 256403 (2005).

[12] M. E. Manley, R. J. McQueeney, B. Fultz, T. Swan-Wood, O. Delaire, E. A. Goremychkin, J. C. Cooley, W. L. Hults, J. C. Lashley, R. Osborn, and J. L. Smith, No role for phonon entropy in the fcc → fcc volume collapse transition in $Ce_{0.9}Th_{0.1}$ at ambient pressure, Phys. Rev. B **67**, 014103 (2003).

[13] P. W. Anderson, Localized magnetic states in metals, Phys. Rev. **124**, 41 (1961).

[14] O. Gunnarsson and K. Schönhammer, Electron spectroscopies for Ce compounds in the impurity model, Phys. Rev. B **28**, 4315 (1983).

[15] Y. Kuramoto and H. Kojima, Self-consistent perturbation theory for dynamics of valence fluctuations, Z. Phys. B: Condens. Matter **57**, 95 (1984).

[16] P. S. Riseborough and J. M. Lawrence, Mixed valent metals, Rep. Prog. Phys. **79**, 084501 (2016).

[17] E. Holland-Moritz and G. H. Lander, Neutron inelastic scattering from actinides and anomalous lanthanides, in *Handbook on the Physics and Chemistry of Rare Earths*, edited by G. R. Choppin, K. A. Gschneidner, L. Eyring, and G. H. Lander (North-Holland, Amsterdam, 1994), Vol. 19, Chap. 130, pp. 1–121.

[18] V. R. Fanelli, J. M. Lawrence, E. A. Goremychkin, R. Osborn, E. D. Bauer, K. J. McClellan, J. D. Thompson, C. H. Booth, A. D. Christianson, and P. S. Riseborough, Q-dependence of the spin fluctuations in the intermediate valence compound $CePd_3$, J. Phys.: Condens. Matter **26**, 225602 (2014).

[19] E. A. Goremychkin, H. Park, R. Osborn, S. Rosenkranz, J.-P. Castellan, V. R. Fanelli, A. D. Christianson, M. B. Stone, E. D. Bauer, K. J. McClellan, D. D. Byler, and J. M. Lawrence, Coherent band excitations in $CePd_3$: A comparison of neutron scattering and ab initio theory, Science **359**, 186 (2018).

[20] E. S. Clementyev, J.-M. Mignot, P. A. Alekseev, V. N. Lazukov, E. V. Nefeodova, I. P. Sadikov, M. Braden, R. Kahn, and G. Lapertot, Dynamic magnetic response in intermediate-valence CeNi, Phys. Rev. B **61**, 6189 (2000).

[21] J. J. Finney and A. Rosenzweig, The crystal structure of CeNi, Acta Cryst. **14**, 69 (1961).

[22] E. S. Clementyev, P. A. Alekseev, M. Braden, J.-M. Mignot, G. Lapertot, V. N. Lazukov, and I. P. Sadikov, Anomalous lattice dynamics in intermediate-valence CeNi, Phys. Rev. B **57**, R8099 (1998).

[23] D. Gignoux and J. Voiron, Pressure-induced first-order transition associated with $4f$ instability in CeNi, Phys. Rev. B **32**, 4822 (1985).

[24] D. Gignoux, C. Vettier, and J. Voiron, First order magnetic transition induced by pressure in ceni, J. Magn. Magn. Mater **70**, 388 (1987).

[25] A. Mirmelstein, E. Clementyev, O. Kerbel, D. Kozlenko, Yu. Akshentsev, V. Voronin, and I. Berger, Pressure effects in CeNi, J. Nucl. Mater. **385**, 57 (2009).

[26] A. Mirmelstein, A. Podlesnyak, Antonio M. dos Santos, G. Ehlers, O. Kerbel, V. Matvienko, A. S. Sefat, B. Saparov, G. J. Halder, and J. G. Tobin, Pressure-induced structural phase transition in CeNi: X-ray and neutron scattering studies and first-principles calculations, Phys. Rev. B **92**, 054102 (2015).

[27] V. N. Lazukov, P. A. Alekseev, E. S. Clementyev, R. Osborn, B. Rainford, I. P. Sadikov, O. D. Chistyakov, and N. B. Kolchugina, Evolution of Ce dynamic magnetic response in Ce$_{1-x}$La$_x$Ni compounds, Europhys. Lett. **33**, 141 (1996).

[28] G. E. Granroth, A. I. Kolesnikov, T. E. Sherline, J. P. Clancy, K. A. Ross, J. P. C. Ruff, B. D. Gaulin, and S. E. Nagler, SEQUOIA: A newly operating chopper spectrometer at the SNS, J. Phys.: Conf. Ser. **251**, 012058 (2010).

[29] M. B. Stone, J. L. Niedziela, D. L. Abernathy, L. DeBeer-Schmitt, G. Ehlers, O. Garlea, G. E. Granroth, M. Graves-Brook, A. I. Kolesnikov, A. Podlesnyak, and B. Winn, A comparison of four direct geometry time-of-fight spectrometers at the Spallation Neutron Source, Rev. Sci. Instrum. **85**, 045113 (2014).

[30] D. L. Abernathy, M. B. Stone, M. J. Loguillo, M. S. Lucas, O. Delaire, X. Tang, J. Y. Y. Lin, and B. Fultz, Design and operation of the wide angular-range chopper spectrometer ARCS at the Spallation Neutron Source, Rev. Sci. Instrum. **83**, 015114 (2012).

[31] V. T. Rajan, Magnetic Susceptibility and Specific Heat of the Coqblin-Schrieffer Model, Phys. Rev. Lett. **51**, 308 (1983).

[32] V. N. Lazukov, E. V. Nefeodova, V. V. Sikolenko, U. Staub, P. A. Alekseev, M. Braden, K. S. Nemkovski, C. Pradervand, I. P. Sadikov, L. Soderholm, and N. N. Tiden, Lattice anomalies in CeNi unstable valence compound, Appl. Phys. A **74**, s559 (2002).

[33] D. Gignoux, F. Givord, R. Lemaire, and F. Tasset, Intermediate valence state of cerium in CeNi, J. Less Common Metals **94**, 165 (1983).

[34] C. Stassis, C. K. Loong, J. Zarestky, O. D. McMasters, R. M. Moon, and J. R. Thompson, Temperature dependence of the field induced magnetic form factor of the intermediate valence compound CePd$_3$, J. Appl. Phys. **53**, 7890 (1982).

[35] P. J. Brown, Magnetic form factors, in *International Tables for Crystallography* (John Wiley & Sons, New Jersey, 2006), Vol. C, Chap. 4.4.5, pp. 454–461.

[36] E. S. Clementyev and A. V. Mirmelstein, Kondo universality, energy scales, and intermediate valence in plutonium, J. Exp. Theor. Phys. **109**, 128 (2009).

[37] M. Loewenhaupt and K. H. Fischer, Valence-fluctuation and heavy-fermion $4f$ systems, in *Handbook on the Physics and Chemistry of Rare Earths*, edited by K. A. Gschneidner and L. R. Eyring (North-Holland, Amsterdam, 1993), Vol. 16, Chap. 105, pp. 1–105.

[38] S. Takayanagi, S. Araki, R. Settai, Y. Ōnuki, and N. Mōri, Pressure effect on the specific heat of CeNi single crystal, J. Phys. Soc. Jpn. **70**, 753 (2001).

[39] E. Balcar and S. W. Lovesey, *Theory of Magnetic Neutron and Photon Scattering* (Oxford University Press, Oxford, 1989).